

TOWARDS DETACHED EDDY SIMULATION MODELLING USING A k -EQUATION TURBULENCE MODEL

Shia-Hui Peng*

Swedish Defence Research Agency, FOI
Computational Physics, Division of Systems Technology
SE-164 90 Stockholm, Sweden
e-mail: peng@foi.se

Web page: <http://www.foi.se/>

*Also at Chalmers University of Technology
Division of Fluid Dynamics, Department of Applied Mechanics
SE-412 96 Gothenburg, Sweden

Key words: Detached Eddy Simulation (DES), Hybrid RANS-LES, k -DES Modelling, k -Equation, Turbulent Length Scale

Abstract. *A detached eddy simulation modelling approach is presented for turbulent flow computations, which is based on the transport equation for turbulent kinetic energy, k (and thus termed **k -DES** model). The model coefficients in the RANS form are calibrated in wall-attached flow computations, and the LES mode is calibrated in the simulation for decaying, homogeneous, isotropic turbulence. To combine the near-wall RANS mode with the off-wall LES mode, the RANS-LES interface is accomplished by means of an adaptation of turbulent length scales invoked in both the production term and the dissipation term of the k -equation. Examples presented for the modelling validation include a fully developed channel flow, a periodic hill flow and a three-dimensional axisymmetric hill flow. The results are compared with available DNS, LES and experimental data, showing reasonable agreement.*

1 INTRODUCTION

Turbulence modelling, as one of the most significant ingredients in simulations of turbulent flows, remains a bottleneck-type problem toward accurate and efficient predictions for complex flows. Great effort has thus been carried on over decades in studies of improved modelling approaches, ranging from classical Reynolds-Averaged Navier-Stokes (RANS) approaches to subgrid-scale (SGS) models in large eddy simulation (LES). In particular, over the recent years increasing attention has been paid to the development of hybrid RANS-LES modelling methods. Benefiting the advantage inherent in LES for accurate resolution of the energetic and large-scale turbulent structures arising in *flow-detached* regions with massive separations, a hybrid RANS-LES method, on the other hand, aims

at alleviating the dense near-wall grid resolution (as should otherwise be required in a full-resolved LES) by using a RANS-type model in the near-wall layer. In the pioneering work by Spalart et al [1, 2], such a modelling approach has been termed Detached Eddy Simulation (DES) with its own specific modelling features, among others, the RANS-LES interface is regulated to be located in the outer edge (or outside) of a wall boundary layer. The DES model employs the Spalart-Allmaras (S-A) [3] one-equation model in both the RANS and LES regions. The DES approach was further extended later by Strelets [4] using Menter's SST two-equation model [5]. Other types of hybrid RANS-LES modelling methods have also been reported over the years, see e.g. in references [6–10].

For convenience of statement, the *DES* modelling is distinguished here from *hybrid RANS-LES* approaches. A hybrid RANS-LES approach is a combination of unsteady RANS (URANS) and LES by means of proper matching of the two, where the LES mode (coupled with the RANS mode) may be located in any desired flow region to attain improved flow resolution and/or numerical grid alleviation. With hybrid RANS-LES modelling, in addition, the RANS mode may be of different type from the LES mode using different turbulence transport equations for various turbulence quantities. For example, a two-equation RANS model may be coupled with a one-equation or a zero equation SGS model (e.g. the Smagorinsky SGS model), and vice versa, provided that the matching between the two is realizable and realistic. The DES approach can be regarded as being a special type of hybrid RANS-LES modelling, with RANS mode adopted only in the wall layer coupled with an off-wall LES mode. Moreover, DES uses the same type of turbulence transport equation(s) for both the RANS and LES modes. The transition/switch from the near-wall RANS region to the off-wall LES region is achieved by means of a *natural* adaptation of turbulent scales inherent in the turbulence transport equation, which aims at enriching, over the RANS-LES matching location/region, the RANS-modelled turbulence in such a way that it is *naturally* compatible to, and matchable with, the LES-resolved turbulence. With the S-A DES by Spalart et al. [1, 2], the RANS-LES interface is accomplished through the eddy viscosity by an adaptation between the RANS length scale and the SGS (in LES mode) length scale.

This work presents a DES modelling approach based on the transport equation for turbulence kinetic energy, k , which is hereafter termed **k-DES**. The k -equation is a *natural* choice in turbulence modelling, since its exact equation is analytically derivable and each term has profound physical properties in the argumentation of modelling. In turning it into a DES-type modelling equation, a methodology similar to the S-A DES model has been adopted for the RANS-LES coupling, that is, through the adaptation of turbulence length scales. In the following sections, we present first the k-DES modelling formulation accompanied with some calibration work for the model coefficients. The model is then applied to several turbulent flows with increasing complexities. The computed results are compared with DNS, LES data and experimental measurements, where available.

2 THE k-DES MODELLING

By applying Reynolds averaging or spatial filtering to the Navier-Stokes equations, the resulting equation system for incompressible flows may be cast in an identical mathematical formulation with the inclusion of the turbulent stress tensor, τ_{ij} , viz.

$$\frac{\partial u_i}{\partial t} + \frac{\partial}{\partial x_j} (u_i u_j) = -\frac{1}{\rho} \frac{\partial p}{\partial x_i} + \nu \frac{\partial^2 u_i}{\partial x_j \partial x_j} - \frac{\partial \tau_{ij}}{\partial x_j} \quad (1)$$

Nonetheless, the turbulent stress term possesses substantially different physical rationale, when experiencing different filtering processes (namely in time or in space). In RANS, the Reynolds stresses, stemmed from the time-averaging process, represent the *mean* effect of turbulence on mean flow motions. With the spatially filtered LES equation system, the subgrid-scale (SGS) stress is involved in the representation of the energy drain between the resolved large-scale turbulent structure and the SGS turbulence. For both the RANS and SGS modelling, the focus is on the approximation of these stresses in order to close the equation system, and to underlay the effect of modelled turbulence (on mean flow motions in RANS and on resolved large-scale flow motions in LES). The most commonly used modelling approach in engineering applications is based on the eddy-viscosity concept, which assumes a linear alignment between the stress tensor and the flow strain rate tensor S_{ij} , namely,

$$\tau_{ij} = -2\nu_e S_{ij} + \frac{2}{3} \delta_{ij} k \quad (2)$$

where ν_e is the eddy viscosity, being generally expressed as the product of a turbulent length scale, \mathcal{L}_μ , and a velocity scale \mathcal{V} . In the present modelling formulation, the turbulent kinetic energy, k , is used to approximate the turbulent velocity scale via. $\mathcal{V} \propto \sqrt{k}$, of which the modelled transport equation takes the conventional form of

$$\frac{Dk}{Dt} = 2\nu_e S_{ij} S_{ij} + \frac{\partial}{\partial x_j} \left[\left(\nu + \frac{\nu_e}{\sigma_k} \right) \frac{\partial k}{\partial x_j} \right] - C_\epsilon \frac{k^{\frac{3}{2}}}{\mathcal{L}_\epsilon} \quad (3)$$

where \mathcal{L}_ϵ is a turbulent length scale for the dissipation term, σ_k and C_ϵ are model constants. With a model constant, C_k , the turbulent eddy viscosity is then given by

$$\nu_e = C_k \sqrt{k} \mathcal{L}_\mu \quad (4)$$

The two turbulence length scales, \mathcal{L}_μ and \mathcal{L}_ϵ , may be justified in proportion to the wall distance in the near-wall RANS region and to the filter width in the off-wall LES region.

Since we intend to use the same transport equation of k for both the RANS and LES modes in the proposed DES approach, the k -equation should then function properly in the context of RANS modelling of near-wall flows. It is known that, for a k -equation RANS model, the length scales, \mathcal{L}_μ and \mathcal{L}_ϵ , behave differently in the vicinity of a wall surface.

This was demonstrated by Chen and Patel in their two-layer RANS model[11]. The Chen-Patel near-wall k -equation model has shown promising performance when dealing with near-wall turbulence in RANS computations. This model has been recently revisited by Temmerman et al. in their hybrid RANS-LES modelling work [8]. With the RANS k -equation, a similar routine as in Chen and Patel [11] is followed here to construct the two turbulent length scales, which are formulated respectively as functions of another length scale, d . The length scale, \mathcal{L}_ε , in the dissipation term of the k -equation reads

$$\mathcal{L}_\varepsilon = \frac{C_\varepsilon}{C_\mu^{3/4}} f_\varepsilon \kappa d \quad (5)$$

where $C_\mu = 0.09$ and $\kappa = 0.418$ is the von Karman constant. The empirical function, f_ε , in Eq. (5) takes the same form as in the Chen-Patel model, namely, $f_\varepsilon = 1 - \exp(-R_d/A)$ with $A = 2\kappa C_\varepsilon C_\mu^{-3/4}$, where $R_d = \sqrt{k}d/\nu$.

The length scale, \mathcal{L}_μ , is formulated as

$$\mathcal{L}_\mu = \frac{C_\mu^{1/4}}{C_k} f_\mu \kappa d \quad (6)$$

where f_μ is another empirical function, which is used to damp the overshoot in the prediction of near-wall turbulence intensities in order to accommodate viscous and wall-damping effects. To attain a correct near-wall asymptotic property, the following damping function, f_μ , has been designed

$$f_\mu = \tanh\left(-\frac{\sqrt{R_d} + R_d}{95}\right) \quad (7)$$

For other model coefficients, we have used $\sigma_k = 1.0$, and for C_ε appearing in the k -equation (Eq. (3)) and C_k in the formulation of ν_e (Eq. (4)), a constant value has been assigned for each with $C_\varepsilon = 1.8$ and $C_k = C_\mu/C_\varepsilon = 0.05$, respectively. When used as a RANS model in the wall layer, the local wall distance, d_w , is employed for the length scale d , namely $d = d_w$. Note that, with the above-presented setting of the model coefficients, the model in its RANS form complies with the local-equilibrium assumption for attached turbulent boundary layer flows.

Figure 1 presents an example, where the k -equation is used as a RANS model in the computation of a turbulent channel flow at a friction Reynolds number of $Re_\tau = 395$. As compared with the DNS data [12], it is shown that the k -equation, used as a near-wall RANS model, is able to produce satisfactory predictions for wall-attached flows.

To incorporate the k -equation in the k-DES modelling, the equation must be turned from the near-wall RANS mode into an off-wall SGS-type model in the LES region, where k is taken as the SGS turbulent kinetic energy. In the LES mode, instead of using the wall distance, the length scale d appearing in Eqs (5) and (6) must be associated to an

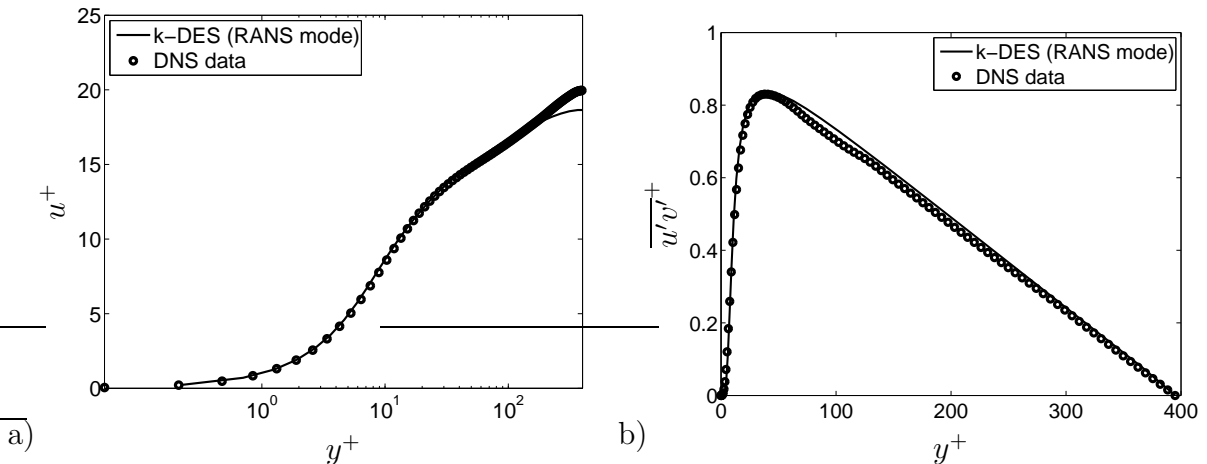


Figure 1: RANS-mode calibration: simulation of turbulent channel flow at $Ra_\tau = 395$ in comparison with DNS data [12]. Note that the results have been normalized by the wall friction velocity. a) Mean streamwise velocity, u^+ . b) Turbulent shear stress, $\overline{u'v'}$.

SGS turbulent length scale, Δ . As often plausibly argued in SGS modelling, the local-equilibrium assumption is applicable for the unfiltered SGS turbulence (particularly in off-wall regions), which consequently indicates that

$$d = \frac{C_\mu^{1/4}}{\kappa \sqrt{f_\mu f_\varepsilon}} \frac{\sqrt{k}}{|S|} \quad (8)$$

where $|S|$ is the magnitude of the flow deformation.

One of the well-calibrated SGS k -equation models in LES is the Yoshizawa model [13], which possesses the same form as Eq. (3) but with different model constants ($C_{k,Y} = 0.07$ and $C_{\varepsilon,Y} = 1.05$). The length scale in the Yoshizawa SGS model takes identically the filter width, namely, $\mathcal{L}_\nu = \mathcal{L}_\varepsilon = \Delta_l$. Using the local-equilibrium assumption, the Yoshizawa model renders

$$\Delta_l = \sqrt{\frac{C_{\varepsilon,Y}}{C_{k,Y}} \frac{\sqrt{k}}{|S|}} \quad (9)$$

The determination of d in the present k -equation model should thus be made comparable to Δ_l as in the well-calibrated Yoshizawa model, when used as an SGS model in LES. Nonetheless, in simulations of decaying, homogeneous, isotropic turbulence (DHIT), it was found that the Yoshizawa SGS model under-estimates the dissipation for *resolved* turbulence energy and that the prediction may be improved by setting $C_{\varepsilon,Y} = 0.6$ [10]. Indeed, an eddy-viscosity based SGS model, which gives good simulations for DHIT, is often too dissipative for flows affected by wall shears. The Smagorinsky SGS model is a typical example as such, which requires a larger value for the model constant (i.e. the

Smagorinsky constant) in DHIT simulations, while for wall-bounded flows the Smagorinsky constant has to be reduced to a smaller value to make the model less dissipative.

Note that the SGS type of the k -equation is used only in *flow-detached* and/or off-wall LES regions for a DES modelling, where the SGS turbulence is expected to be more isotropic with a well-resolved LES resolution. The k -equation in the form of its SGS mode is thus also calibrated in the simulation of DHIT. Apart from the same set of model constants and functions as for the RANS mode, the SGS k -equation has used the following formulation for the SGS turbulence length scale, d ,

$$d = C_{kdes}\Delta \quad \text{and} \quad \Delta = \frac{2\delta V^{1/3}\Delta_{max}}{(\delta V^{1/3} + \Delta_{max})} \quad (10)$$

where C_{kdes} is a model constant and $C_{kdes} = 0.62$, being calibrated from the simulation of DHIT, δV is the control volume of a local node and Δ_{max} is the local maximum cell size, $\Delta_{max} = \max(\Delta_x, \Delta_y, \Delta_z)$.

The value of model constant, C_{kdes} , is calibrated from the simulation of DHIT based on the experiment by Comte-Bellot and Corssin[14]. The initial field was generated using the experimental data measured at $t = 42$ [15]. Figure 2 a) presents the LES-simulated energy spectra at $t = 98$ and $t = 171$ using the present SGS k -equation model with $d = C_{kdes}\Delta$ and $C_{des} = 0.62$. Also given in Figure 2 b) is the LES-resolved energy decaying with the time. As seen, the present k -equation, being turned into an SGS model, is able to produce reasonable predictions, as compared with the experimental data and with the result computed using the Smagorinsky model.

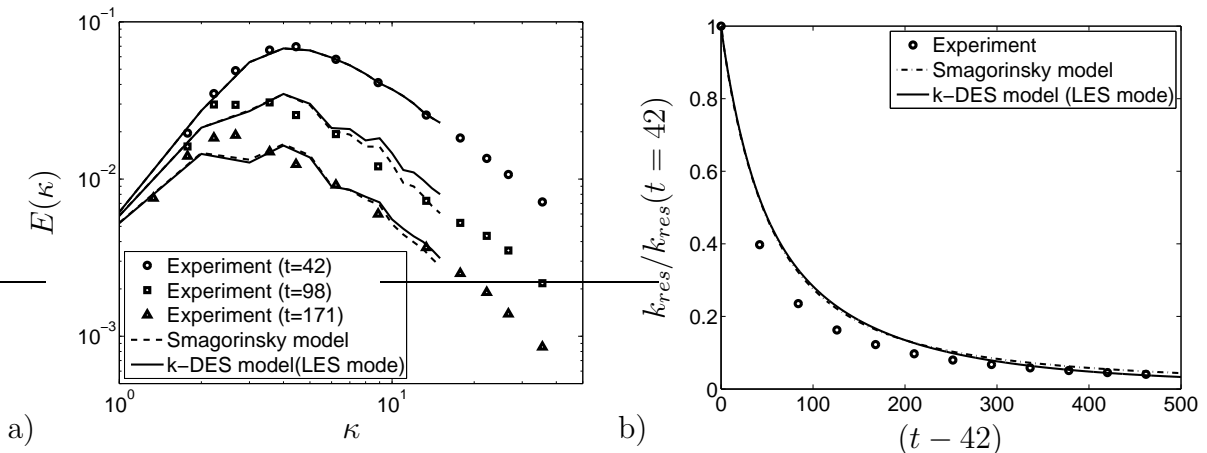


Figure 2: LES-mode calibration (with $C_{kdes} = 0.62$): simulation of decaying, homogeneous, isotropic turbulence in comparison with the Smagorinsky model and experimental data. a) Computed energy Spectra. b) Resolved turbulence energy decaying with time.

The transition/switch between the RANS mode and the LES mode based on the same k -equation is attained through the length scale, d , which is computed by the following

relation in the k-DES model,

$$d = \min(d_w, C_{kdes}\Delta) \quad (11)$$

Apart from the model constant C_{kdes} and the determination of Δ (with Eq. (10)), the RANS-LES switching relation, Eq. (11), is the same as in the S-A DES model [1]. Note that the length scale d is invoked in both the production and dissipation terms in the k -equation, as shown in Eqs (5) and (6). In the wall layer with a thickness of d_w , the k -equation performs with its RANS form, and is adjusted to an SGS model away from this layer. As demonstrated in Figure 1, the k -equation in its RANS form (i.e. $d \equiv d_w$) is able to appropriately model the attached wall layer from the viscous sublayer up to the fully turbulent log-layer. When switched to the LES mode (i.e. $d \equiv C_{kdes}\Delta$), the k -equation functions as an SGS model with $C_{kdes} = 0.62$, rendering appropriate SGS modelling features similar to the Yoshizawa SGS k -equation model [13].

Nonetheless, it was found that in computations of flows with wall shears the k-DES model is somewhat too dissipative in the LES region. As mentioned above, this has encountered in calibrations for other SGS models based on eddy viscosity concept. Indeed, a DHIT-calibrated model constant may induce too much energy dissipation when the same model constant is applied to wall-bounded flows. Instead of re-calibrating the model constant for shear flows to limit possible over-estimation of the dissipation, we introduce an additional turbulent length scale, which has been appeared in Eq. (8), namely $l_s = \sqrt{k}/|S|$. As the local-equilibrium assumption is applied, this length scale is comparable to the filtering length scale, and is equivalent to the Taylor microscale over the RANS-LES interface where the velocity scale, \sqrt{k} , is a representative scale for both RANS-modelled turbulence and SGS turbulence. The length scale, l_s , is used to further regulate \mathcal{L}_μ and \mathcal{L}_ε in the k-DES model. As a consequence, the length scales, \mathcal{L}_μ and \mathcal{L}_ε , are replaced, respectively, with L_μ and L_ε , viz.

$$\begin{aligned} L_\mu &= \min\left(\mathcal{L}_\mu, \frac{\alpha\sqrt{k}}{|S|}\right) \\ L_\varepsilon &= \max\left(\mathcal{L}_\varepsilon, \frac{\beta\sqrt{k}}{|S|}\right) \end{aligned} \quad (12)$$

As L_μ and L_ε approach respectively the minimum and maximum values, Eq. (12) suggests that $\alpha\beta = C_\varepsilon/C_k$ in order to comply with the local-equilibrium assumption. We have set $\alpha = \beta = 6.0$ in all the computations presented in the section below.

Thorough investigation has not yet been completed on the effect of the RANS-LES switching location in connection to the near-wall meshing. Nonetheless, it is expected that the present k-DES model should not impose strong restriction on the RANS-LES interfacing location. As argued, the present k -equation as an SGS model is similar to the well-calibrated Yoshizawa model. The model should thus be applicable in full resolved

LES for wall-bounded flows. For the k-DES modelling, when combined with the near-wall RANS mode, it seems plausible to comp up with a conjecture that the simulation may not be so sensitive to the location of the RANS-LES interface, being placed in the outer edge of the boundary layer or in the boundary layer. Certainly, this by no means implies that the RANS-LES interface may penetrate to the buffer layer or below, where small-scale but energetic streaky structures exist and should be modelled with the RANS mode for the purpose of DES modelling.

As with other DES and hybrid RANS-LES models, one of the main purposes with the present k-DES model is to alleviate the near-wall grid resolution in the wall-tangential directions. The mesh spacing in the wall-normal direction should remain comparable to that in LES or in low-Reynolds number RANS modelling to resolve large near-wall gradients, for which the first node must be placed in the viscous sublayer with $y^+ \sim 1$. Apart from the control volume of a local node, δV , the characteristic filter width, Δ , in the LES mode is justified by the local maximum cell size in the wall-tangential direction (see Eq. (10)). With a sufficiently refined mesh, it is obvious that the k-DES model returns to its LES mode in the overall computational domain with $d \equiv C_{kdes}\Delta$.

The present work is intended to present the k-DES modelling approach as an alternative DES model, and to examine its performance in turbulent flow computations. Comprehensive modelling validation and calibration will be carried on in simulations of both turbulent incompressible and compressible flows. In the following section, we present the results computed with the k-DES model for some test cases from an ongoing EU project DESider (cf. <http://cfd.me.umist.ac.uk/desider/>).

3 RESULTS AND DISCUSSION

In this section, the k-DES model is examined in computations of three turbulent flows, of which the results are compared with DNS, full-resolved LES and experimental data, where available. We consider first a fully developed turbulent channel flow to examine the performance of the k-DES model for wall-attached flows. The model is then applied to a turbulent channel flow with hills periodically mounted on the channel bottom wall with homogeneous transverse boundaries. In this case, the separation of the mean flow on the backside of the hill is two-dimensional. In the last test case, a three-dimensional hill flow is considered, where an axisymmetric hill is mounted on the bottom wall of a duct (wind tunnel in experiment). The turbulent separation on the leeward side of the hill is three-dimensional. These test cases, with increasing complexities, should shed light on different aspects of the present k-DES modelling approach.

In the results presented below, a fluctuating quantity of the resolved field is denoted by $\phi' = \phi - \langle \phi \rangle$, and the symbol, $\langle \cdot \rangle$, is used to denote the quantities obtained from time-averaging and spatial-averaging over the homogeneous directions for the turbulent channel flow and the periodical hill flow. For the 3D hill flow, this denotation indicates only time averaging.

All the computations presented in this work has been carried out with an incompressible

flow solver, which solves the incompressible Navier-Stokes equations using a pressure-based scheme. The solver employs the second-order central differencing scheme for all terms based on the finite volume method with structured grid. The second-order Crank-Nicholson scheme is used for the temporal discretization. A Poisson equation is derived for the pressure, which is solved using an efficient multigrid solver. The time-dependent, discretized equation system is solved using an implicit, fractional step technique with a non-staggered grid arrangement. Detailed information on the solver can be found in Davidson and Peng [6].

3.1 Turbulent channel flow

As a typical test case, fully developed turbulent channel flows have often been used in the calibration of turbulence models of various type. It should be noted that, for DES model, as termed in the name (detached eddy simulation) by Spalart et al. [1], one takes the merit of the LES mode when modelling *flow-detached* regions, where the flow undergoes massive separation characterized by turbulence mixing and vortical motions. Turbulence in such regions are more isotropic than in near-wall regions with wall shears. To properly resolve large-scale structures in these regions, the mesh resolution must be sufficiently fine. When applied to channel flows, the off-wall LES region is not detached but rather affected by shears. The DES modelling in this case is viewed as a type of wall model in LES, as highlighted by Nikitin et al. in their channel flow computations with the S-A DES model [16].

We consider here the turbulent channel flow computed by Piomelli et al. with full-resolved LES [17]. The Reynolds number, Re_τ , based on the wall friction velocity and the half channel height is about 2000. The computational domain has dimensions of 2π , 2 and π in the streamwise (x), vertical (y) and spanwise (z) directions, respectively. The mesh is uniformly distributed in the x and z directions, while being clustered near the wall in the y direction. A mesh with $64 \times 64 \times 32$ cells has been employed, giving $y_1^+ \approx 1.13$ and $\Delta x^+ = \Delta z^+ \approx 196$. Apparently, the wall-parallel grid resolution, Δx^+ and Δz^+ , is much larger than a full LES resolution. By adding a pressure force in the streamwise momentum equation, which ensures a correct Re_τ , periodic boundary condition is imposed on the streamwise boundaries, which is also used for the spanwise boundaries.

As shown in Figure 3, the model shows some typical features of a hybrid RANS-LES modelling for wall-attached flows. Near the wall where the RANS mode is used, the mean streamwise velocity is reasonably reproduced, as compared with the LES data. Note that the RANS-LES interface occurs at a wall distance of about $y^+ \simeq 75$. In the range of $y^+ < 200$, the time-averaged streamwise velocity is well reproduced, as compared with the LES data. Away from this wall distance, it is over-estimated. This is due to the mesh resolution in this region, which is too coarse in the wall-parallel direction to enable accurate LES. Similar predictions for channel flows were observed in the work by Nikitin et al. using the S-A DES model [16]. Nevertheless, the predicted total turbulent shear stress (the modelled part plus the resolved part) agrees well with the LES data. As

shown in Figure 3 b), a major part of the turbulent shear stress in the RANS region is modelled, which decreases in the LES region but remains a relatively large contribution to the total turbulent shear stress up to about $y^+ \simeq 310$, after which the resolved part becomes dominant. It should be noted that, in the distribution of the turbulent shear stress, a small peak appears at about the RANS-LES interface. This has been brought about by the modelled part due to the mesh used. At the interface, the RANS length scale (in terms of the wall distance, d_w) is switched to the SGS length scale (i.e. $C_{kdes}\Delta$). The wall distance for each node changes (continuously) in accordance with the grid stretching ratio in the wall-normal direction. The SGS length scale (justified in terms of local control volume and maximum cell size) at the interface may not follow this "continuous" mesh stretching and has consequently induced a small peak. This can be easily removed by using a well-designed mesh. As shown below, such a peak is not present in the computation for other test cases.

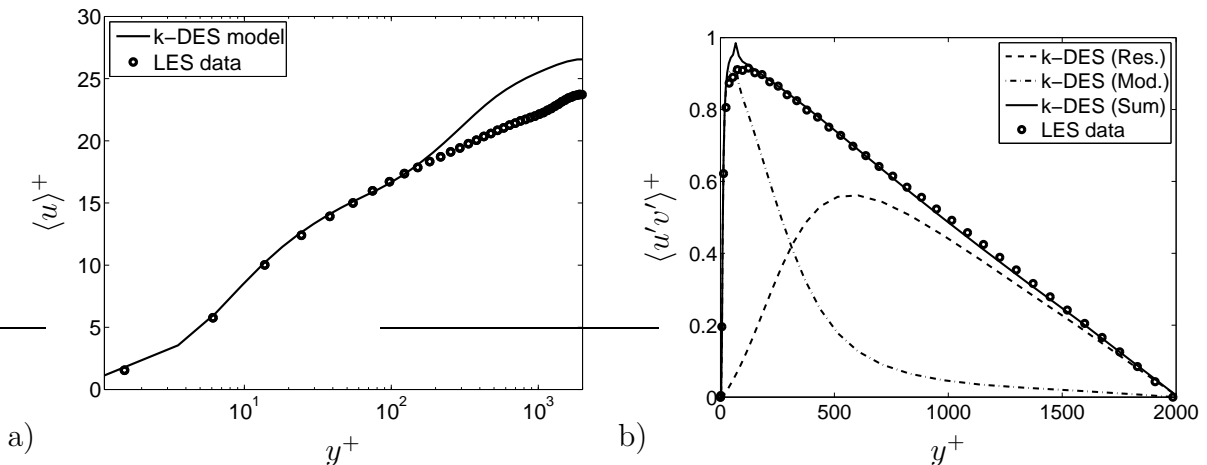


Figure 3: Simulation of channel flow at $Re_\tau = 2000$ in comparison with full-resolved LES data [17]. a) Resolved streamwise velocity, $\langle u \rangle^+$. b) Resolved turbulent shear stress, $\langle u'v' \rangle^+$.

3.2 Periodic hill flow

The k-DES model is further examined in the simulation for a turbulent channel flow with hills periodically mounted on the bottom wall. A periodic segment is taken in the computation with $L_x \times L_y \times L_z = 9h \times 3.036h \times 4.5h$, where $h = 0.028$ is the height of the hill. The Reynolds number based on the bulk velocity above the hill crest, U_b , and the hill height is $Re = 10595$. The mesh used in the present computation has $112 \times 64 \times 48$ cells. The computed results are compared with the LES data by Temmerman et al. [18], in which a $196 \times 128 \times 186$ mesh was employed to resolve the wall turbulence.

Figure 4 a) illustrates the mean flow streamlines simulated with the k-DES model. For comparison, the streamlines obtained with the S-A DES is also plotted in Fig. 4 b). As seen, both models are able to reproduce reasonably well the separation bubble arising on

the leeside of the hill shortly after the hill top and being reattached downstream after the foot of the hill. The LES claims that the separation starts at $x_s = 0.22h$ with a downstream extension to $x_r = 4.72h$.

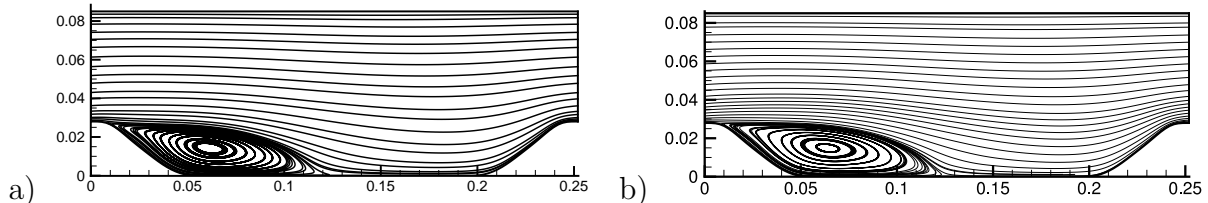


Figure 4: Simulation of periodic hill flow. Illustration of mean flow streamlines. LES produces separation point at $x_s = 0.22h$ and re-attachment location at $x_r = 4.72h$ [18]. a) k-DES model with $x_s = 0.22$ and $x_r = 4.65$. b) S-A DES model with $x_s = 0.20$ and $x_r = 4.84$.

In Figure 5, the distribution of velocity computed with the k-DES is compared with the LES data, extracted from four locations covering the leeside separation bubble. The comparison is made respectively for the streamwise velocity in Figure 5 a) and for the vertical velocity in Figure 5 b). As compared with the LES data, the k-DES results are similar to those obtained with the S-A DES model. For the mean vertical velocity, $\langle v \rangle$, the prediction with the k-DES model is slightly better than with the S-A DES model. Corresponding to the good prediction of the separation bubble, both models have reasonably produced the backflow in the separation region, as shown in Figure 5 a) for the streamwise velocity profiles at locations $x/h = 1.0$ and $x/h = 2.0$. The vertical velocity is however under-estimated at $x/h = 1.0$ and over-predicted at $x/h = 2.0$ in comparison with the LES data.

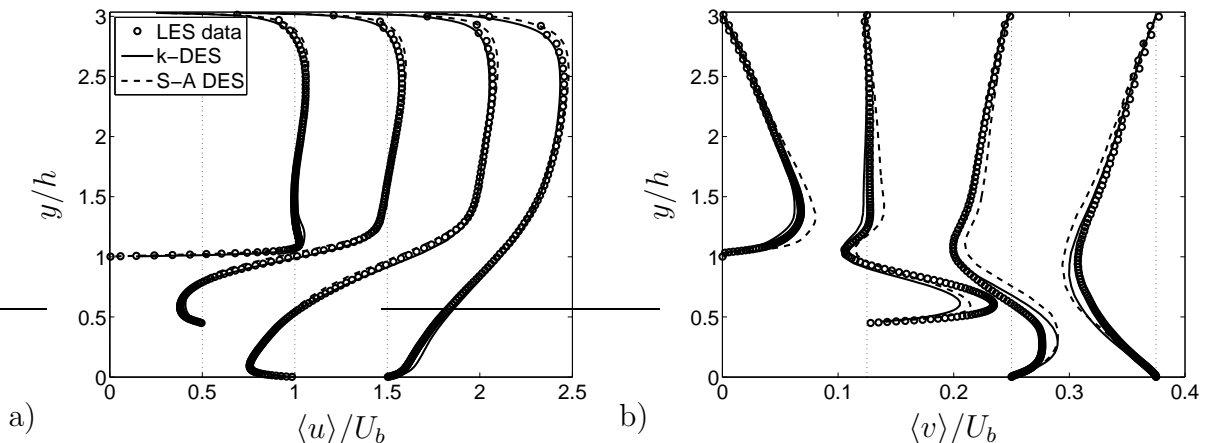


Figure 5: Simulation of periodic hill flow. Vertical profiles for the mean velocities plotted at stations $x/h = 0, 1.0, 2.0$ and 5.0 (from left to right), respectively. a) Mean streamwise velocity. b) Mean vertical velocity.

The prediction for the turbulence statistics is presented in Figure 6, where the vertical profiles for the turbulent kinetic energy and turbulent shear stress are plotted. The total turbulent kinetic energy and the total turbulent shear stress are taken in the comparison with the LES data, as shown in Figures 6 a) and b), respectively. They have been computed as the sum of the resolved part and the modelled part. To clarify the contribution of the modelled part, Figures 6 c) and d) have plotted, respectively, the vertical distributions for the modelled turbulence kinetic energy, k_{mod} , and the modelled turbulent shear stress, $\langle \tau_{12} \rangle$. These figures use the same scale as in Figures 6 a) and b) for comparison. Note that the S-A DES does not invoke a model for the turbulence kinetic energy, of which the modelled contribution is thus zero, as shown in Figure 6 c). While both models render negligible contributions due to the modelled turbulent shear stress, the modelled turbulent kinetic energy with the k-DES model is marginally sensible in the shear layer above the separation bubble and in the near-wall region. In general, the DES results are shown to be in reasonable agreement with the LES data. Nevertheless, the total turbulent kinetic energy and the total turbulent shear stress (and thus their resolved counterparts) have been under-estimated by both DES models in the shear layer above the bubble at location $x = h$, whereas these quantities are somewhat over-predicted at the downstream station $x = 5h$ after the reattachment of the separation bubble.

3.3 Three-dimensional axisymmetric hill flow

The flow over an axisymmetric 3D hill is characterized by 3D separation on the leeward side of the hill, for which the experimental measurement was conducted by Simpson et al. [19]. This case was chosen as a test case at the 11th ERCOFTAC Workshop on Refined Turbulence Modelling (Gothenburg, Sweden, 7-8 April 2005). It was shown from the workshop that RANS models in general give rise to largely erroneous predictions of the flow, particularly, in the region over the leeward side of the 3D hill and downstream thereafter. LES and hybrid RANS-LES models have shown generally improved predictions in reproducing the mean flow properties and turbulence statistics. The results presented at the ERCOFTAC workshop indicate that this flow is a rather challenging type for modelling the 3D turbulent separation and for simulating downstream flow properties. There have been some recent computations for this flow using LES and hybrid RANS-LES modelling approaches, see e.g. in references [20–22].

In this test case, the Reynolds number based on the height of the hill, h , and a nominal freestream velocity, U_c , is $Re_h = 1.3 \times 10^5$. The computational domain (Figure 7 a)) has dimensions of $L_x \times L_y \times L_z = (-x_0 + 8.2)h \times 3.205h \times 11.67h$. The inflow section is located at $x_0 = -4.11h$ upstream from the center of the hill, where the origin of the coordinate system is set. The computation uses a mesh with $128 \times 80 \times 96$ cells in the x , y and z directions, respectively. To highlight the flow feature, in Figure 7 b) the time-averaged surface friction pattern is illustrated, which has been computed with the present k-DES model. It is detected that the modelled separation on the leeward side of the hill occurs at about $x/h = 0.52$, and being reattached at about $x/h = 2.21$ (shortly after the foot of

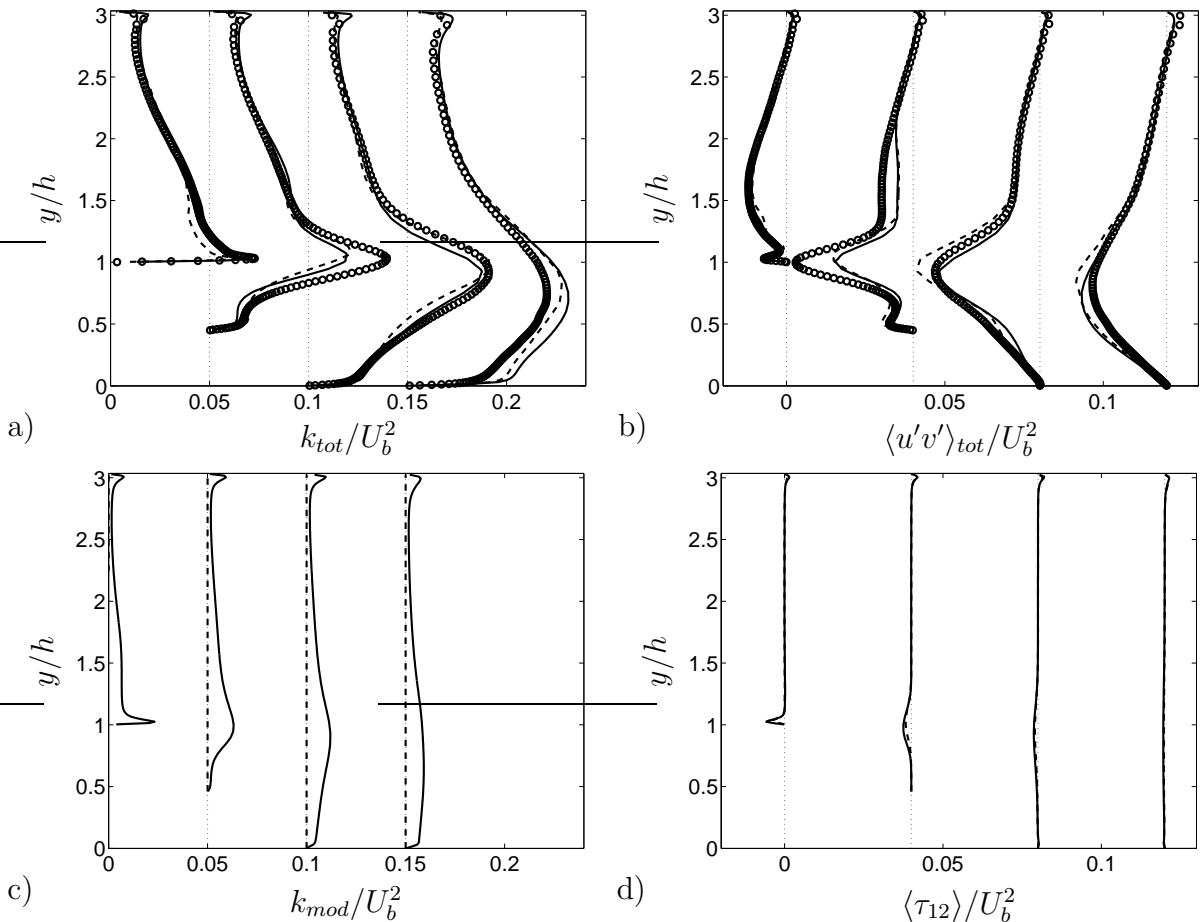


Figure 6: Simulation of periodic hill flow. Vertical profiles for time-averaged turbulence statistics, plotted at the same locations and using the same legend as in Figure 5. a) Total turbulent kinetic energy, $k_{tot} = k_{res} + k_{mod}$. b) Total turbulent shear stress, $\langle u'v' \rangle_{tot} = \langle u'v' \rangle_{res} + \langle \tau_{12} \rangle$. c) Modelled turbulent kinetic energy, k_{mod} . d) Modelled turbulent shear stress, $\langle \tau_{12} \rangle$.

the hill). Downstream of the separation bubble, the flow is fully recovered on the lower bottom wall at about $x/h = 4.0$, as disclosed in the prediction by the k-DES model.

In the computation, the mean flow profile measured experimentally at $x = 0$ with the hill removed is prescribed on the inflow section at $x = -4.11h$. The turbulent inflow condition is approximated using the flow properties at the outflow section by a recycling and re-scaling method, which was described in details in Peng [23]. On the top and bottom boundaries no-slip wall conditions are imposed and symmetric conditions on the spanwise side boundaries. The time step used in the computation is $\Delta t \simeq 0.017h/U_c$. Before the statistic analysis is carried out, the running with a time period of about $72L_x/U_c$ is discarded, after which the time-averaging starts and is carried on for a period of more than $260h/U_c$.

Figure 8 presents some vertical profiles for the mean velocities and turbulence statis-

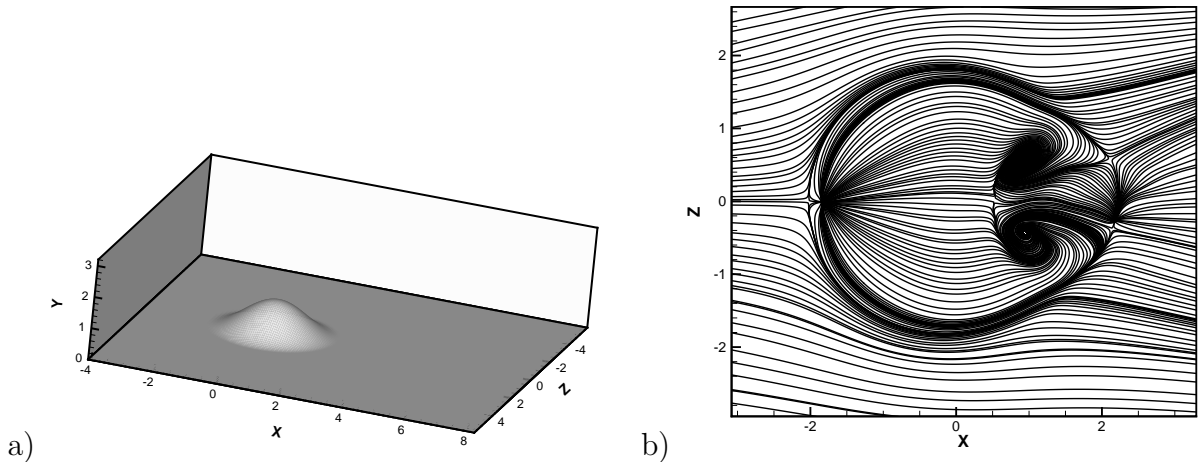


Figure 7: Three-dimensional axisymmetric hill flow. a) Sketch of the computational domain and geometry. b) Illustration of time-averaged surface friction pattern over the hill, simulated with the k-DES model.

tics. They are taken from a downstream (of the hill) section at $x/h = 3.69$, where the experimental measurement was conducted at different z/h -stations over the spanwise z -direction. The vertical distributions measured at four stations have been used for comparison, taken respectively at $z/h = 0$, $z/h = -0.33$, $z/h = -0.65$ and $z/h = -1.30$. As shown, the mean streamwise velocity is predicted better at the mid-section ($z = 0$) than at the side stations, where this velocity is more sensibly over-predicted in the boundary layer. The predicted spanwise velocity agrees reasonably well with the measured data, in particular at station $z/h = -1.30$. For the turbulence statistics, as indicated in Figure 8 c), the model pronounces a sensible deficit for the resolved turbulent kinetic energy in the outer part of the boundary layer at stations $z/h = 0$, $z/h = -0.33$ and $z/h = -0.65$, in comparison with the measured data. This suggest that the resolved turbulent fluctuations are under-estimated in the shear layer, partly due to the grid resolution in this region, where under-predictions occur also in the resolved turbulent shear stress, as shown in Figure 8 d). Nevertheless, the turbulent shear stress has been reasonably resolved in the near-wall region. The addition of the modelled part to the turbulent kinetic energy and to the turbulent shear stress may help to some extent improve the comparison with the measured data in the outer shear layer of the boundary layer. The modelled contribution is however not retrieved in the present analysis. It is noted here that the turbulent kinetic energy and turbulent shear stress are also marginally under-predicted in the shear layer for the periodic hill flow (see Figures 6 a) and b) at station $x/h = 1.0$). This may suggest that the LES mode has rendered too much energy dissipation from the resolved scales to the modelled SGS turbulence. Note that the energy flux from the resolved to unfiltered structures is related to the grid resolution. With a too coarse mesh in a region where the flow undergoes large flow deformation (e.g. in the shear layer), the resolved turbulence

energy may become over-dissipated, and leading to inaccurate predictions. It is anticipated that a refined grid resolution in the shear layer should improve the predictions.

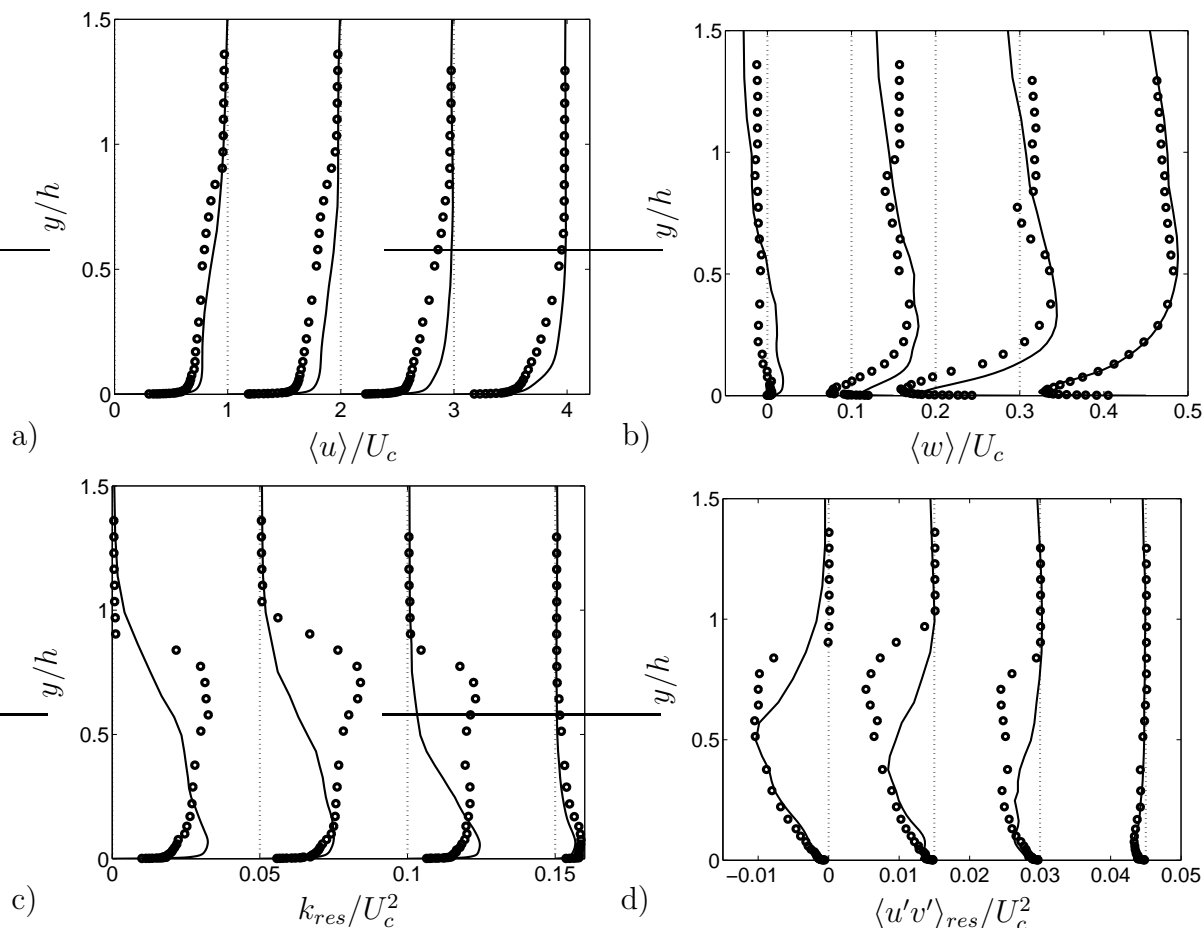


Figure 8: Simulation of 3D axi-symmetric hill flow. Vertical profiles at section $x/h = 3.69$, plotted respectively at locations $z/h = 0$, $z/h = -0.33$, $z/h = -0.65$ and $z/h = -1.30$ (from left to right) in comparison with experimental data. a) Time-averaged streamwise velocity. b) Time-averaged spanwise velocity. c) Resolved turbulent kinetic energy. d) Resolved turbulent shear stress.

In Figure 9, the mean velocity field plotted over the leeward side of the hill is highlighted in comparison with the experimental measurement on section $z = 0$. The dotted line indicates the location where the streamwise velocity is zero. As shown, the model produces the streamwise extension of the separation bubble that is similar to the measured velocity field, while the predicted "thickness" of this bubble seems somewhat larger than the measured schematic, for which the predicted backflow in the bubble may be relatively extensive. The k-DES prediction indicates that the flow reattaches at about $x_r = 2.21h$,

which similar to the experimental observation [19].

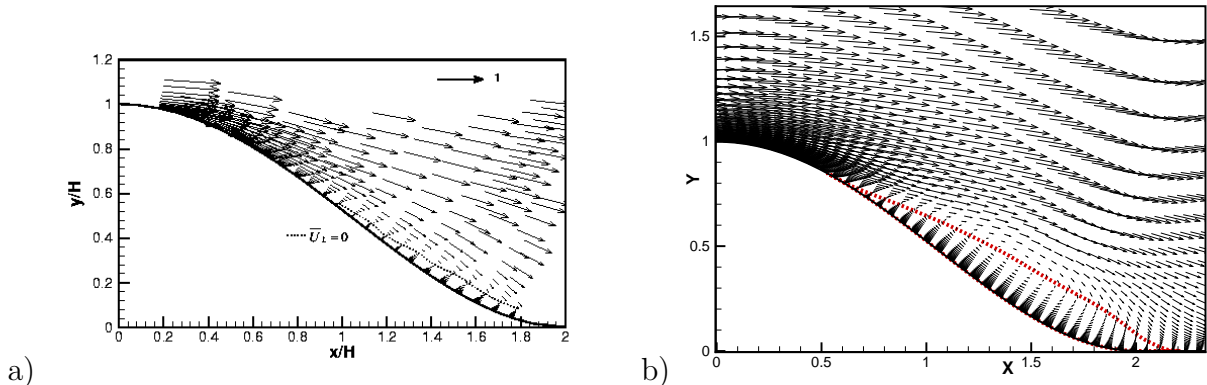


Figure 9: Simulation of 3D axis-symmetric hill flow. Illustration of the separation bubble on the leeward side of the hill on the $z = 0$ plane. The dotted line in both figures indicates zero values of streamwise velocities. a) Measured velocity field [19]. b) Computed velocity field with the k-DES model, which discloses the separation point at $x_s = 0.52h$ and reattachment location at $x_r = 2.21h$.

4 CONCLUSIONS

A DES modelling approach, the k-DES model, is presented for turbulent flow computations, which is based on the transport equation for turbulence kinetic energy, k . The RANS form combined in the k-DES model incorporates correct asymptotic properties when integrated to the wall surface. It is shown that the RANS mode is able to produce satisfactory predictions for wall-attached flow. The k -equation is switched from the near-wall RANS mode to an SGS model in the LES region and solving for the SGS turbulence kinetic energy. The LES mode is calibrated in the simulation for decaying, homogeneous, isotropic turbulence, showing reasonable performance in reproducing the energy spectra and the turbulence energy decaying with time, as compared with experimental data and with the Smagorinsky SGS model.

Similar to the S-A DES model, the RANS-LES interface with the k-DES model is accomplished by means of the adaptation between the RANS length scale from the near-wall region and the SGS length scale from the off-wall LES region. In the computation of three turbulent flows with increasing complexities, the k-DES model has shown encouraging performance. The mean flow is reasonably predicted, as compared with available DNS, LES and experimental data. The flow separation (for both the 2D and 3D cases considered) has been reproduced reasonably well. The results obtained with the model are similar to (or even better than) the predictions computed with other hybrid RANS-LES methods. For the resolved turbulence statistics in the cases with flow separation, some discrepancies between the k-DES prediction and the LES (or measured) data are observed in the region where the free shear layer arises (above the bubble). This is, to a large extent, attributed

to the grid resolution used in the present computations, which is relatively coarse and has consequently made the dissipation over-estimated for the resolved turbulence energy.

The k-DES model is built on the basis of the transport equation for the turbulent kinetic energy, of which its modelling has probably the least controversies as compared with other scale-determining turbulence transport equations in the context of both RANS and SGS modelling. In addition, the exact k -equation is theoretically derivable so that the modelled terms can be traced back to their exact counterparts in *a priori* test with DNS and/or experimental data. Moreover, apart from the correct near-wall asymptotic property for the RANS modelling, for the LES mode the SGS modelling argumentation is similar to other well-calibrated SGS models. In the future work, comprehensive analysis on the k-DES model will be carried out on issues such as the effect of grid resolution and near-wall meshing, as well as the effect of the location for the RANS-LES interface.

Acknowledgment

The work was partially supported by the EU project DESider, which is a collaboration between Alenia, ANSYS-AEA, Chalmers University, CNRS-Lille, Dassault, DLR, EADS Military Aircraft, EUROCOPTER Germany, EDF, FOI, IMFT, Imperial College London, NLR, NTS, NUMECA, ONERA, TU Berlin, and UMIST. The project is funded by the European Community represented by the CEC, Research Directorate-General, in the 6th Framework Programme, under Contract No. AST3-CT-2003-502842.

REFERENCES

- [1] P. R. Spalart, W-H. Jou, M. Strelets, and S. R. Allmaras. Comments on the feasibility of les for wings and on a hybrid rans/les approach. In C. Liu and Z. Liu, editors, *Advances in DNS/LES: Proceedings of the First AFOSR International Conference on DNS/LES*. Greyden Press, Columbus, 1997.
- [2] P. R. Spalart. Strategies for turbulence modelling and simulations. In W. Rodi and D. Laurence, editors, *Engineering Turbulence Modelling and Experiments 4*, pages 3–17. Elsevier Science, 1999.
- [3] P. R. Spalart and S. R. Allmaras. A one-equation turbulence model for aerodynamic flows. AIAA Paper 92-0439, Reno, 1992.
- [4] M. Strelets. Detached-eddy simulation of massively separated flows. AIAA 2001-0879, Reno, 2001.
- [5] F. R. Menter. Eddy viscosity transport equations and their relation to the $k - \varepsilon$ model. *ASME J. of Fluids Engineering*, 119:876–884, 1997.
- [6] L. Davidson and S.-H. Peng. Hybrid LES-RANS modelling: A one-equation SGS model combined with a $k - \omega$ model for predicting recirculating flows. *International Journal for Numerical Methods in Fluids*, 43:1003–1018, 2003.

- [7] F. Hamba. An attempt to combine large eddy simulation with the $k - \varepsilon$ model in a channel flow computation. *Theoret. Comput. Fluid Dynamics*, 14:323–336, 2001.
- [8] L. Temmerman, M. Hadziabdic, M. Leschziner, and K. Hanjalic. A hybrid two-layer urans-les approach for large eddy simulation at high reynolds numbers. *Int. J. Heat and Fluid Flow (in press)*, 2004.
- [9] P. Batten, U. Goldberg, and S. Chakravarthy. Interfacing staistical turbulence closres with large-eddy simulation. *AIAA J.*, 42:485–492, 2004.
- [10] S.-H. Peng. Hybrid RANS-LES modelling based on zero- and one-equation models for turbulent flow simulation. In *Proceedings of 4th Int. Symp. Turb. and Shear Flow Phenomena*, volume 3, pages 1159–1164, 2005.
- [11] H. C. Chen and V. C. Patel. Near-wall turbulence models for complex flows including separation. *AIAA J.*, 26:641–648, 1988.
- [12] J. Kim, P. Moin, and R. Moser. Turbulence statistics in fully developed channel flow at low reynolds number. *Journal Fluid Mechanics*, 177:133–166, 1987.
- [13] A. Yoshizawa. Statistical theory for compressible shear flows, with the application to subgrid modeling. *Phys. Fluids*, 29:2152–2164, 1986.
- [14] G. Comte-Bellot and S. Corssin. Simple Eulerian time correlation of full- and narrow-band velocity signals in grid-generated, 'isotropic' turbulence. *J. Fluid Mech.*, 48:273–337, 1971.
- [15] M. Strelets, M. Shur, and Co-workers. Calibration of the subgrid eddy-viscosity models on the basis of les of decaying homogeneous isotropic turbulence. Report, New Technologies and Services, Russia, 2004.
- [16] N. V. Nikitin, F. Nicoud, B. Wasistho, K. D. Squires, and P. R. Spalart. An approach to wall modeling in large-eddy simulations. *Phys. Fluids*, 12:1629–1632, 2002.
- [17] U. Piomelli, E. Balaras, H. Pasinato, K. Squires, and P. Spalart. The inner-outer layer interface in large-eddy simulations with wall-layer models. *Int. J. Heat and Fluid Flow*, 24:538–550, 2003.
- [18] C. Mellen L. Temmerman, M. Leschziner and J. Frlich. Investigation of wall-function approximations and subgrid-scale models in large eddy simulation of separated flow in a channel with streamwise periodic constrictions. *Int. J. Heat and Fluid Flow*, 24:157–180, 2003.
- [19] R. L. Simpson, C. H. Long, and G. Byun. Study of vortical separation from an axisymmetric hill. *Int. J. Heat and Fluid Flow*, 23:582–591, 2002.

- [20] N. Li, C. Wang, A. Avdis, and M.A. Leschziner. Large eddy simulation of separation from a three-dimensional hill and comparison with second-moment-closure RANS modelling. In *4th Int. Symp. on Turbulence and Shear Flow Phenomena*, volume 1, pages 331–336, Williamsburg, USA., 2005.
- [21] S. Benhamadouche, J. Uribe, N. Jarrin, and D. Laurence. Large eddy simulation of asymmetric bump on structured and unstructured grids, comparisons with RANS and T-RANS models. In *4th Int. Symp. on Turbulence and Shear Flow Phenomena*, volume 1, pages 325–330, Williamsburg, USA.
- [22] L. Davidson and S. Dahlström. Hybrid LES-RANS: Computation of the flow around a three-dimensional hill. In *Engineering Turbulence Modelling and Measurements 6*, Eds. W. Rodi, M. Mulas, pages 319–328, 2005.
- [23] S.-H. Peng. Algebraic hybrid RANS-LES modelling applied to incompressible and compressible turbulent flows. AIAA Paper 2006-3910. San Francisco, 2006.